IEEE Access
Multidisciplinary ⋮ Rapid Review ⋮ Open Access Journal

Received May 6, 2020, accepted May 30, 2020, date of publication June 2, 2020, date of current version June 12, 2020.

Digital Object Identifier 10.1109/ACCESS.2020.2999449

Facial Image Privacy Protection Based on Principal Components of Adversarial Segmented Image Blocks

JINGJING YANG[1,2,3], JIAXING LIU[2], AND JINZHAO WU[1,3,4,5]

[1]Chengdu Institute of Computer Applications, Chinese Academy of Sciences, Chengdu 610041, China
[2]School of Information Science and Engineering, Hebei North University, Zhangjiakou 075000, China
[3]University of Chinese Academy of Sciences, Beijing 100049, China
[4]Guangxi Key Laboratory of Hybrid Computation and IC Design Analysis, Guangxi University for Nationalities, Nanning 530006, China
[5]School of Computer Science and Electronic Information, Guangxi University, Nanning 530000, China

Corresponding author: Jinzhao Wu (yjr78z@gmail.com)

This work was supported in part by the National Natural Science Foundation of China under Grant 61772006, in part by the Science and Technology Major Project of Guangxi under Grant AA17204096, in part by the Key Research and Development Project of Guangxi under Grant AB17129012, in part by the Fund Project of Hebei North University under Grant JYT2019016, the Financial Supported Projects of Zhangjiakou Science and Technology under Grant 1911016C-9, in part by the Natural Science Foundation of Hebei Province of China, and in part by the Special Fund for Bagui Scholars of Guangxi.

ABSTRACT The features in facial images, which are utilized for a variety of technological applications, pose a significant privacy concern for users. This paper proposes a method for protecting privacy in facial images based on the principal components of adversarial segmented image blocks. Generative adversarial network parameters are compressed by segmenting the facial images into blocks and extracting the principal components of the segmented image. The generator and discriminator in the generative adversarial network then generate images similar to the original facial images; the facial images generated by the generator, as-driven by the target recognition network, markedly different from the original facial images. As the generator, discriminator, and target recognition network compete with each other, minor perturbation is added to the principal components of the facial images to protect the users' privacy and prevent distinct face-related features of the images from being easily extracted. Experimental results show that the proposed method outperforms other similar methods in terms of generated image quality, operation speed, and target recognition network accuracy.

INDEX TERMS Facial image privacy protection, generative adversarial network, principal components, adversarial samples.

I. INTRODUCTION

Modern facial image recognition technology is relatively unaffected by problems with lighting [1], [2], or occlusion [3], [4]. It has been widely applied in the Internet of Things, security, mobile payment, and many other applications. Passenger vehicles, for example, use face recognition for keyless starting [5] – merchants use face recognition for online payment [6], and buildings use face recognition for access control [7]. Facial features come with significant privacy concerns [8]. According to incomplete statistics, the number of ''selfie'' photos shared daily by users on social media now exceeds one billion [9], [10]. Most social networks impose no limits on the downloading of facial images. To this effect, the leakage of facial images poses a significant threat. If features in the facial images are extracted by lawbreakers and data mining is performed to obtain user-related privacy information, the users' property may become severely insecure [11]–[13]. Protecting the facial image features can effectively preserve user privacy. It is necessary to secure these features from extraction before allowing it to be published while retaining as much of the original information as possible to ensure the readability and practicality of the image.

There are advantages and drawbacks to the existing methods for facial image privacy protection. Methods based on

The associate editor coordinating the review of this manuscript and approving it for publication was Ahmed Farouk.

encryption [14], [15], for instance, require burdensome calculations, have poor real-time performance, do not allow for the direct use of data, and are restricted within an application scope. Methods based on image filtering [16] significantly damage the original face information and do not guarantee image availability. Anonymity-based methods [17], [18] are susceptible to privacy leakage due to similar or background knowledge attacks.

In 2013, Szegedy *et al.* [19] proposed the "adversarial samples" concept wherein a small amount of perturbation is added to sample data to cause the target model to generate incorrect classification with high confidence. Wide range protection of similar image privacy protection methods then emerged, including the Fast Gradient Sign Method (FGSM) [20], Adversarial Patch [21], and One Pixel Attack [22]. Xiao *et al.* [23] proposed the generation of adversarial examples with adversarial networks (AdvGAN) based on generative adversarial networks in 2018. Adding a small amount of perturbation to the image with a generative adversarial network (GAN) causes the target network to consistently produce the wrong classification and is robust against both white- and black-box attacks. He *et al.* [24] and Wu *et al.* [25] proposed networks similar to AdvGAN for the generation of facial privacy images, where the target network is misled to perform a misclassification while ensuring the availability of facial images.

The paper proposes a method for facial image privacy protection based on principal components of adversarial segmented image blocks. We add tiny perturbations to the facial images. When the facial images are published on the cloud service platform such as social media, the recognition network of potential lawbreakers will recognize errors. As a result, the data mining of users by potential criminals will not be successful while protecting the users' privacy and maintaining the practicability of pictures. The main contributions are as follows.

1. A tiny amount of perturbation is added to the principal components of facial images to ensure that the image as-generated is fully available.

2. The principal components of the segmented facial images are extracted to minimize the generator input parameters and accelerate the running speed of the process.

3. A target face recognition network is added in the competition between the generator and the discriminator for misleading, which gives the generated facial image a different label than the original image.

4. Peak Signal to Noise Ratio (PSNR) constraint conditions is added to ensure the generated facial image is similar to the original facial image pixel-wise.

II. RELATED WORK

Goodfellow *et al.* [20] proposed a fast gradient sign method (FGSM) in 2014. The gradient of the input image is obtained by calculating the target category, and then the sign function of the gradient is obtained. Finally, the obtained results are added to the original image as the antagonistic perturbations to obtain the antagonistic samples that can confuse the recognition network. Liu *et al.* [35] in 2018 and Linardos *et al.* [36] in 2019 applied FGSM in face privacy protection. Both can protect the privacy of images while maintaining high quality. However, FGSM has the disadvantage that the added perturbations can be easily removed, such as using the median filtering method. So FGSM is not in our consideration.

Influenced by AdvGAN proposed by Xiao *et al.* [23], He *et al.* [24] proposed a picture privacy protection algorithm based on the generated adversary network (PriGAN) in 2019. The U-NET network structure is combined with the generated adversarial network (GAN) to realize image privacy protection. However, the resulting privacy images have a checkerboard effect. In 2019, Wu *et al.* [25] proposed a new architecture for image Privacy protection named Privacy-Protective-GAN (PP-GAN), adding validators and adjustment modules explicitly designed for face recognition to achieve de-identified output with a similar structure based on a single input. However, the features of the generated privacy image are different from the original image, so it is not suitable for some application scenarios that require high practicability of the image. We will propose a method that is superior to other similar methods in terms of image quality, operation speed, and target recognition network accuracy.

III. PRINCIPAL COMPONENT ANALYSIS

Principal Component Analysis [26] (PCA) is often used to reduce the dimensionality of data and extract the main features of images. PCA works based on relatively little operating data and with a relatively small memory footprint, which makes it accessible in many fields, including image classification.

A. BACKGROUND

N facial images are given $X = \{X_1, X_2, \cdots\cdots X_N\}$ for any facial image $X_i \in R^{m\times n}$. Singular Value Decomposition (SVD) for PCA dimensionality reduction is applied to X_i as follows:

$$X_{i,m,n} = U_{m,m}\Lambda_{m,n}V^T_{n,n} \approx U_{m,k}\Lambda_{k,k}V^T_{k,n} \tag{1}$$

where $U_{m,m}$ is the left singular matrix of X_i, which can compress the X_i number of rows, $V_{n,n}$ is the right singular matrix of X_i, which can compress the X_i number of columns, and $\Lambda_{m,n}$ is the singular value of X_i that has been sorted by size. As the sum of the first k singular values accounts for more than 95% of the sum of all singular values, the left singular matrix of the first k dimensions can be multiplied by the singular value and right singular matrix, which is approximately equal to the original image X_i. This results in image dimensionality reduction.

B. PERTURBATION OF PRINCIPAL COMPONENTS

For convenience, let the compression matrix be $Z = \Lambda V^T$. Then, (2) holds for any facial image X_i.

$$X_i = U_{m,m}Z_{m,n} \approx U_{m,k}Z_{k,n} \tag{2}$$

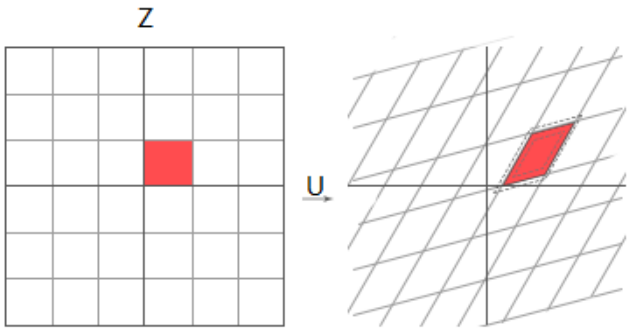

FIGURE 1. Perturbation of asymmetric matrix transformation.

X_i can be regarded as a linear transformation of matrices U and Z. The multiplication of matrices U and Z is actually an asymmetric transformation of the elements in Z and the transformation of a single element Z into a single element in X_i, as marked with a solid red line in Figure 1. As shown in (3), the elements in the matrix U may be subjected to slight perturbation; the results of the asymmetric transformation then also generate corresponding fluctuations in various directions, as shown in Figure 1. Possible fluctuations in the transformation of a single element in Z (as marked with a dotted line in the figure) also cause the corresponding pixel point in the facial image X_i to change slightly.

$$U' = U + N \tag{3}$$

where the matrix N is a perturbation matrix with the same dimensions as U.

C. PERTURBATION ANALYSIS

The calculated adversarial sample of U was actually slight perturbation with the base coordinates of the principal components. The elements in U have been standardized, and the value range is within $[-1, 1]$, which contributes to the iterative operation of the algorithm for perturbation calculation. The principal component contains the main features of the facial image X_i. Accumulating perturbation to the principal component via linear transformation can speed up the generation of facial images with privacy protected. As the principal components contain the main features of the facial image X_i, when the perturbation is added to the main features, the perturbation in the generated facial image with privacy protected cannot be easily filtered out. That is, the image can not be quickly restored.

For the generated set of facial images with protected privacy $X' = \{X'_1, X'_2, \cdots\cdots X'_N\}$, in the case of $X'_i \in X'$, (4) is true.

$$X'_i = U'Z + E = X_i + NZ + E \tag{4}$$

where E is the error between X_i that was subjected to PCA transformation and X'_i. To ensure the availability of the facial privacy image, the difference between the facial image X_i and the privacy image X'_i should be invisible to the naked eye; that is, the error and perturbation matrix should be minimal.

Let f be the fitting function of the target face recognition network. To protect the privacy of the facial image for f, the difference between the facial image X_i and the privacy image X'_i should be maximized, as shown in (5).

$$\begin{aligned} &\min ||X_i - X'_i||_2 \\ &s.t.\, f(X_i) \neq f(X'_i) \end{aligned} \tag{5}$$

D. IMAGE SEGMENTATION

The facial image X_i usually has high dimensionality. Here, X_i was segmented into sub-blocks of $p \times q$ as follows:

$$X_i = \begin{pmatrix} X_{11} & \cdots & X_{1q} \\ \vdots & \ddots & \vdots \\ X_{p1} & \cdots & X_{pq} \end{pmatrix} \tag{6}$$

Establishing the facial privacy image X'_i is equivalent to adding perturbation to the left singular matrix U of the sub-block X_i, as shown in (7). As the left singular matrix U of the sub-block is much smaller in dimensions than the left singular matrix U of the entire facial image X_i, the number of parameters in the network can be reduced. The sub-blocks obtained by segmentation also increase the number of trained samples and decrease the complexity of the problem, thus accelerating the perturbation-solving process.

$$X'_i = \begin{pmatrix} (U_{11} + N_{11})Z_{11} & \cdots & (U_{1q} + N_{1q})Z_{1q} \\ \vdots & \ddots & \vdots \\ (U_{p1} + N_{p1})Z_{p1} & \cdots & (U_{pq} + N_{pq})Z_{pq} \end{pmatrix} \tag{7}$$

IV. MATH FACIAL IMAGE GENERATION NETWORK OF ADVERSARIAL SEGMENTED IMAGE BLOCK PRINCIPAL COMPONENTS

As the data distribution of the facial privacy image X'_i is infinitely approximated to the original facial image X_i, a GAN can be applied to solve the facial privacy image that satisfies (5).

A. BACKGROUND

The GAN is a deep learning model proposed by Goodfellow *et al.* [27] in 2014. The loss function of G and D is minimized by finding the Nash equilibrium point between the generator G and the discriminator D, so that the data generated from G approximates the real data.

Goodfellow *et al.* [27] first proposed the Conditional Generative Adversarial Net (CGAN), where parameters guide the generation of data under supervised learning. GAN techniques proposed by Wang *et al.* [29], Xiao *et al.* [23], He *et al.* [24], and Wu *et al.* [25] are improved variations of CGAN. The facial image generation network of the adversarial segmentation principle components can also be considered a supervised learning process. This differs from the CGAN process as a supervised network is added to the generative adversarial network to drive classification errors in the generated facial images.

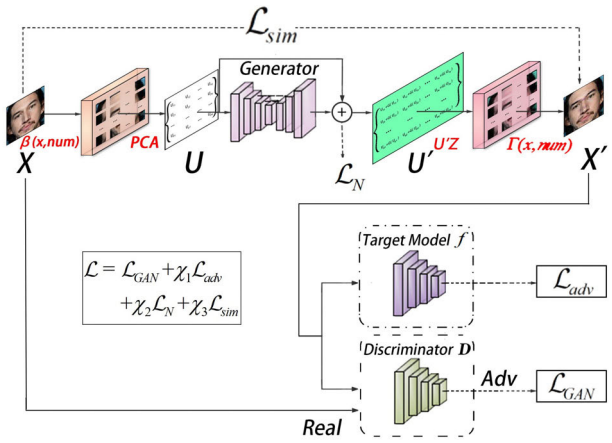

FIGURE 2. PcadvGAN network architecture.

TABLE 1. PcadvGAN flow.

The flow of facial image privacy protection method based on adversarial segmented image block principal components
while a number of training iterations:
Simple X_i from X;
The image segmentation function $\beta(x,num)$ is segmented X_i into sub-blocks of $p\times q$;
The left singular matrix is obtained by SVD decomposition of the sub-blocks of $p\times q$, and the first k singular values are taken to obtain the left singular matrix set U and compressed matrix set Z;
The matrix set U of the sub-blocks serves as the initial parameters and is input to the generator G for training and obtaining the output perturbation matrix set N;
The perturbation matrix set N is substituted into (3) to obtain U';
U' is substituted into (2) to obtain the set of sub-blocks $p\times q$ after the addition of perturbation;
The sub-block set uses (7) and the image merging function $\Gamma(x,num)$ to obtain the privacy image X_i';
X_i' and X_i are input into the discriminator D for training and discriminating whether the data distribution of X_i' is consistent with that of the original face data X_i;
X_i' is input into the target face recognition network f to judge whether it is consistent with the label of the original face data X_i;
end

B. NETWORK ARCHITECTURE

The structure of the privacy-protected facial image generation network based on the principal components of the adversarial segmented image blocks is shown in Figure 2. This is the so-called "PcadvGAN," which includes a generator G, a discriminator D, and a target face adversarial recognition network f. The left singular matrix set U of the facial image sub-block X_i was used as the input of the generator G, as the GAN convergence rate is faster when the distribution of the initial data is similar to the distribution of the real data. The flow of the proposed method is shown in Table 1.

As shown in Table 1, the role of the image segmentation function $\beta(x, num)$ is to segment the image matrix. The x in the parameters represents the original image and $num = p \times q$ represents the number of image blocks. The label in the original matrix is retained after segmentation and represents the set of block images in the image merging function $\Gamma(x, num)$. The matrix is restored according to the label of the block matrix in the original image.

C. LOSS FUNCTION

The role of the discriminator D is to distinguish the difference between X' and the original facial image X, thus ensuring close consistency in data distributions between X' and the original facial image X. The first loss function of PcadvGAN is expressed as follows:

$$\mathcal{L}_{\text{GAN}} = \mathbb{E}_X \log D(X) + \mathbb{E}_{X,X'} \log(1 - D(\Gamma(X')|G(\beta(X)))) \tag{8}$$

In (8), the original facial image X participates in the generation of the facial privacy image X', which is essentially a set N to which adversarial sample perturbation generated by the generator is added. The X' with the added adversarial sample perturbation then trains the discriminator D together with the original facial image X. The generator G is reversely updated, according to the probability that the outputs of the samples by the discriminator D are true, until the loss function $\mathcal{L}_{\text{GAN}}$ reveals the optimal value. The error E between X subjected to PCA transformation and X' as the sample perturbation set N is thus minimized.

The target face recognition network f is denoted as a network model that has been properly trained using the dataset at high accuracy. The parameters would not be updated during the training process. The proposed method (Table 1) can thus be applied to combat black-box and white-box attacks on the samples [30]. As shown in (9), f receives a privacy image X' as an input. If it belongs to the classification t of the original facial image X, it returns a higher loss value; if it belongs to a misleading classification, it returns a lower loss value, thereby ensuring the privacy of the facial image X'.

$$\mathcal{L}_{\text{adv}} = \mathbb{E}_{X'} \ell_f(X', t, t') \tag{9}$$

In the white-box environment and with purposeless label training, the target face recognition network f can return a set of classification labels closest to the classification t of the original facial image X in Euclidean distance. One of the labels is selected for training to accelerate the GAN convergence rate.

Theoretically, the output range of the elements in the set U of left singular matrices is $[-1, 1]$. In actuality, the pixel value of each image varies considerably, and so the output range may be much smaller. As a result, as shown in (10), the perturbation range of the generator G output can be appropriately reduced:

$$\mathcal{L}_N = \mathbb{E}_U (\rho \|G(U)\|_2) \tag{10}$$

where ρ is the coefficient. Adjusting the size of ρ according to the value range of U can further reduce the GAN training time.

To ensure that the generated face privacy image X' approximates the original facial image X at the pixel level, as shown in (11), a pixel-level constraint is added, and the PSNR is utilized to evaluate the similarity of the two images.

$$\mathcal{L}_{sim} = \max\left(\mathbb{E}_{X,X'}\left(\frac{(40 - PSNR(X, X'))}{40}\right), 0\right) \quad (11)$$

When the PSNR output value is higher than 40 dB, the two facial images are highly approximate [38], [39]. When the output value ranges from 30-40 dB, the generated image X' is acceptable despite slight distortion [40]. To facilitate feedback from the loss function, the PSNR output can be restricted to $[-1, 1]$, that is, $\mathcal{L}_{sim} \leq 0.25$ means that the generated facial image X' is within an acceptable range.

The loss function of the entire PcadvGAN is:

$$\mathcal{L} = \mathcal{L}_{GAN} + \chi_1\mathcal{L}_{adv} + \chi_2\mathcal{L}_N + \chi_3\mathcal{L}_{sim} \quad (12)$$

where χ_1, χ_2, χ_3 are the respective hyperparameters of the loss function.

V. EXPERIMENT

A. EXPERIMENTAL ENVIRONMENT

The hardware environment for the experimental test was comprised of an Intel i7-8700K CPU with 32GB DDR4 memory and an NVIDIA GeForce GTX 1080 graphics card.

The software environment was a Windows10 64 bit operating system running the Google Tensorflow framework. Codes were written in Python. The VGGFACE and VGGFACE2 public datasets were used as the basis for the experiment. A black-box environment can be converted to a white-box environment by training distillation models and other methods [23], [24], so a white-box environment was used in this test with unlabeled attacks; in this case, the service provider actively protected the privacy of the users' facial images. The target face recognition network f could return a set of the closest classification labels of the original facial image, thus accelerating convergence. After several tests, the optimal results were identified when the hyper-parameters $\chi_1 = 1.0$, $\chi_2 = 30$, $\chi_3 = 0.1$, $num = 4$, and k were set to retain 98% of the singular values. These settings were used for all subsequent experiments. When $num > 4$, the best results need more epochs and more time. $num = 4$ is the best setting in this experiment.

AdvGAN has been proven superior to FGSM, Opt, and other methods [23]. PriGAN is also suitable for the generation of face privacy images. Accordingly, we focused various performance indicators of the proposed PcadvGAN, PriGAN and AdvGAN in conducting our analysis.

B. NETWORK STRUCTURES OF GENERATOR AND DISCRIMINATOR

The discriminator uses three convolutional layers to extract the features of the input data. All layers use LeakyRelu as the activation function. Two of the convolutional layers use Instance Norm, thus improving the stability of the model and accelerating the convergence speed. The last fully-connected layer uses Sigmod as the activation function. Figure 3 shows a diagram of this structure.

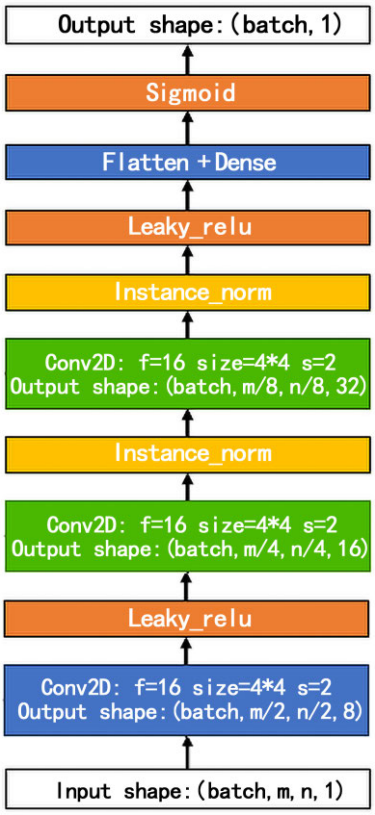

FIGURE 3. Discriminator network structure.

The generator network structure is shown in Figure 4. The input data passes through three convolutional layers and three deconvolutional layers and is output via the Tanh activation function. Instance Norm and LeakyRelu were imposed in each of the convolutional and deconvolutional layers here to enhance the robustness of the generator. LeakyRelu is an unsaturated activation function, which gives all negative values a non-zero slope to solve the problem of gradient disappearance. Four layers of residual blocks were also added between the convolutional layer and the deconvolutional layer to increase the generator's network depth. The network structure of the residual block is shown in Figure 5. It consists of two convolutional layers and Instance Norm, and its activation function is Relu.

C. EXPERIMENT AND ANALYSIS OF FACIAL IMAGES

The VGGFACE and VGGFACE2 datasets are already properly trained in high-accuracy models [31]–[34]. The properly trained face recognition model was defined here as the target face recognition network f. The basic accuracy of each target face recognition network f as-observed in this experiment listed in Table 2.

We divide the training set, development set, and test set according to the 98:1:1 ratio. There are 2622 people with different identities in the VGGFACE datasets, and there are

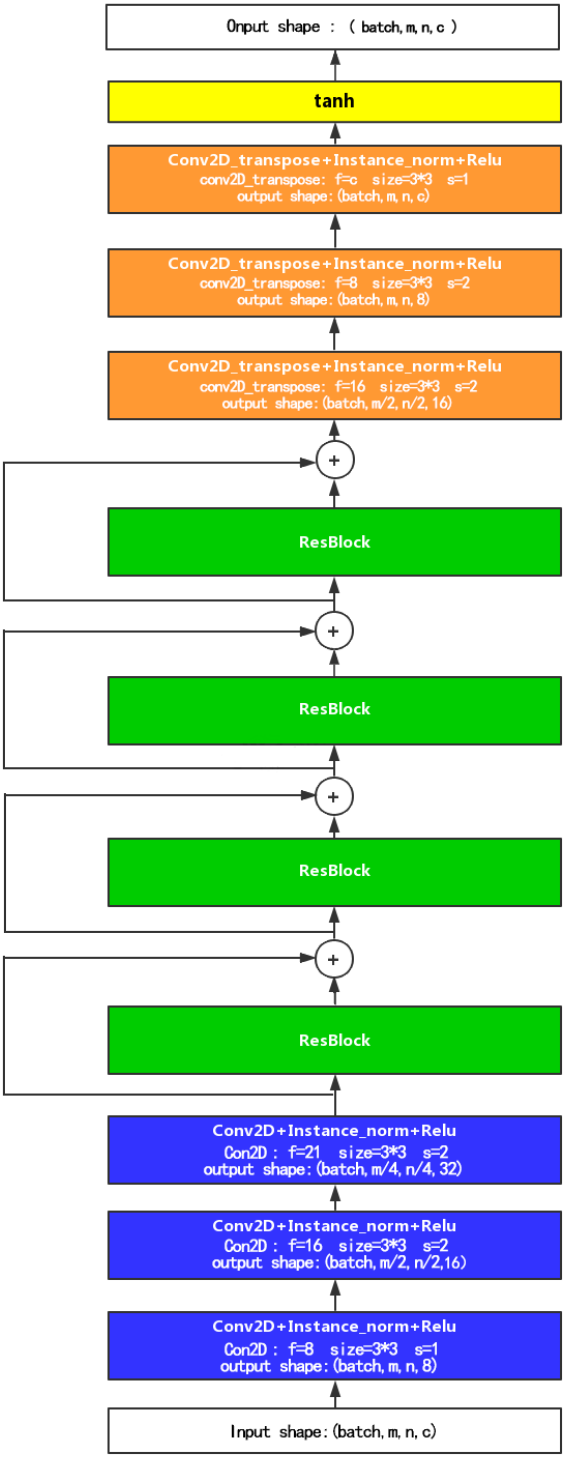

FIGURE 4. Generator network structure.

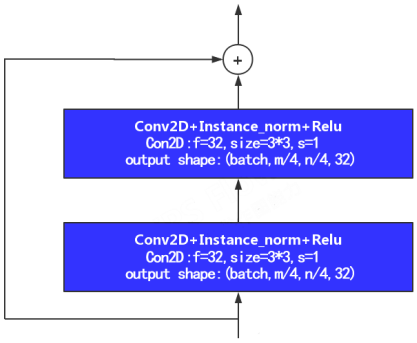

FIGURE 5. Resblock structure.

TABLE 2. Basic accuracy of target face recognition network f (%).

f and dataset	Accuracy
VGGFace(VGG16)	97.27
VGGFace2(Resnet50)	94.70
VGGFace2(Senet50)	95.60

TABLE 3. The accuracy rate of the target face recognition network f for generating facial privacy images (%).

Method	VGGFace(VGG16)	VGGFace2(Resnet50)	VGGFace2(Senet50)
AdvGAN	0	0	0
PriGAN	0	0	0
PcadvGAN	0	0	0

2.6 million face images. We take 2.55 million face images as the training set, 0.026 million face images as the development set, and 0.026 million face images as the test set. There are 9131 people with different identities in the VGGFACE2 datasets, and there are 3.31 million face images. We take 3.24 million to face images as the training set, 0.033 million face images as the development set, and 0.033 million face images as the test set. The training process of PcadvGAN iterating 2,000 epochs is shown in Figure 6. L-noise represents the size of the perturbations $\mathcal{L}_N$, and L-sim is $\mathcal{L}_{sim}$. The Acc (the accuracy of the target faces recognition network for generating face privacy images) is inversely proportional to the perturbations output $\mathcal{L}_N$ of the generator. The recognition accuracy Acc is also inversely proportional to the quality loss of facial image $\mathcal{L}_N$. At the beginning of the training process, we set a large initial value for the perturbations. The values of $\mathcal{L}_N$, $\mathcal{L}_{sim}$ and Acc vary widely. In order to reduce $\mathcal{L}_N$ and $\mathcal{L}_{sim}$, the accuracy rate of Acc fluctuation frequency is very high. With the increase of training times, PcadvGAN gradually learned to balance the relationship between the three. After 600 training sessions, it is obvious that the fluctuation frequency of Acc, $\mathcal{L}_N$ and $\mathcal{L}_{sim}$ gradually decreases and finally reaches a stable state. Eventually, PcadvGAN learned to reduce the values of $\mathcal{L}_N$ and $\mathcal{L}_{sim}$ while maintaining an Acc equal to 0. In figure 6, we highlighted two advantages in 2000 training sessions in green boxes.

After AdvGAN, PriGAN, and PcadvGAN iterated 2,000 epochs, the accuracy rate of the target face recognition network f for generating face privacy images was as shown in Table 3. AdvGAN, PriGAN, and PcadvGAN both reduced the accuracy rate of the target face recognition network f to 0%, which in practice would protect the privacy of the facial image.

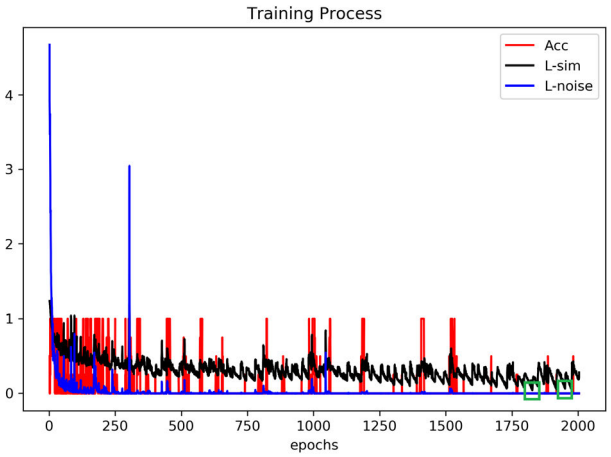

FIGURE 6. Training process.

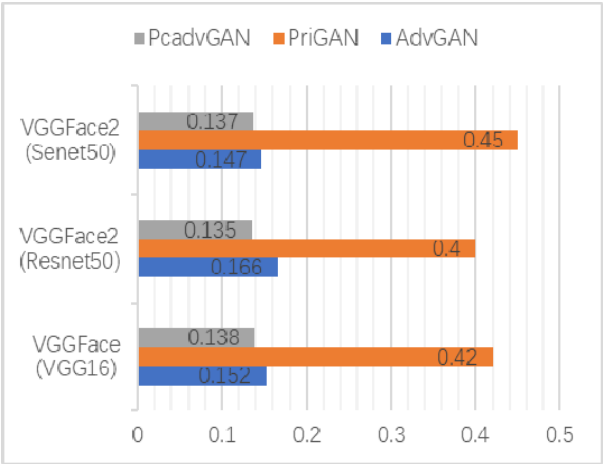

FIGURE 7. Comparison of original facial image and generated facial privacy images $\mathcal{L}_{sim}$.

In the case where the accuracy rate of the generated face privacy image Acc was reduced to 0% for the target face recognition network f, the original facial image and the generated facial privacy images were taken to calculate the image similarity using (11) as shown in Figure 7.

Using Acc drop as 0% as the benchmark, PriGAN $\mathcal{L}_{sim} > 0.25$, the generated facial privacy images were visually unacceptable. When AdvGAN and PcadvGAN $\mathcal{L}_{sim} < 0.25$, the generated facial privacy images were visually acceptable. Due to the loss function $\mathcal{L}_{sim}$ of PcadvGAN, the quality of these privacy images was better than those generated by AdvGAN and PriGAN.

The visual contrast between the generated facial privacy images and the original images are shown in Figure 8. Most features of the original facial images are retained and well visible to the human eye, thereby ensuring the "availability" of the generated image.

The visual contrast between facial images generated by AdvGAN, PriGAN, PcadvGAN, and original images are shown in Figure 9. The color and contrast ratio of facial images generated by PriGAN has changed a lot, and the

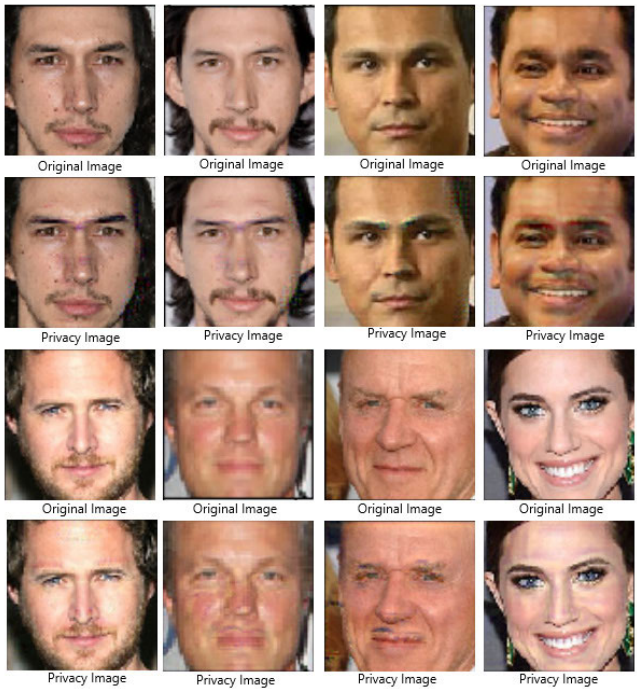

FIGURE 8. Visual comparison between facial images generated by PcadvGAN and original facial images.

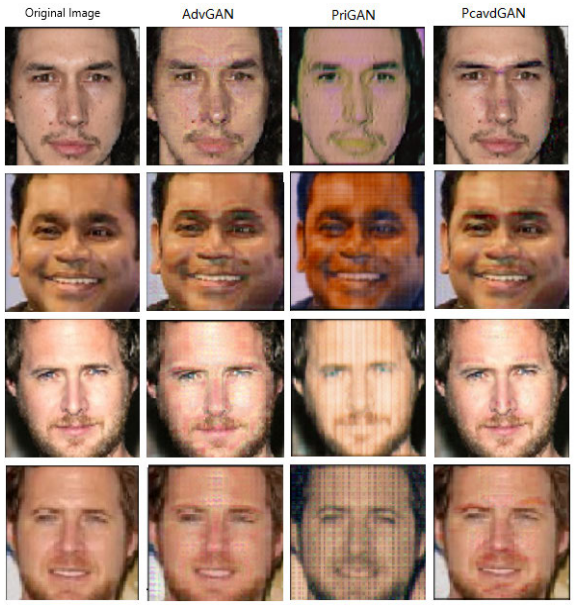

FIGURE 9. Visual comparison between facial images generated by AdvGAN, PriGAN, PcadvGAN and original images.

chessboard effect of the images is obvious. The facial images generated by AdvGAN and PcadvGAN both can ensure the "availability." Moreover, compared with AdvGAN and PriGAN, the quality of the facial images generated by PcadvGAN is better.

The pixel contrast between the generated and original facial images are shown in Figure 10. The perturbation interfered with the primary features of all faces and was not easily

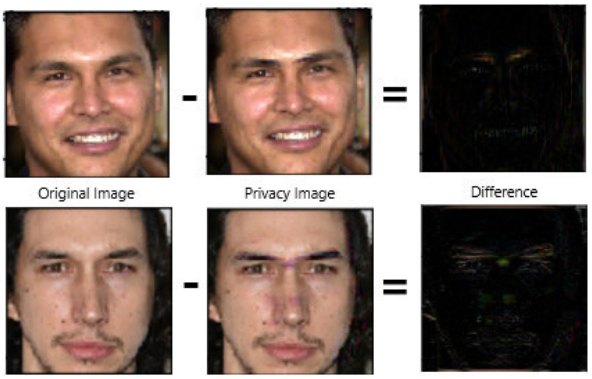

FIGURE 10. Pixel comparison between PcadvGAN-generated and original facial images.

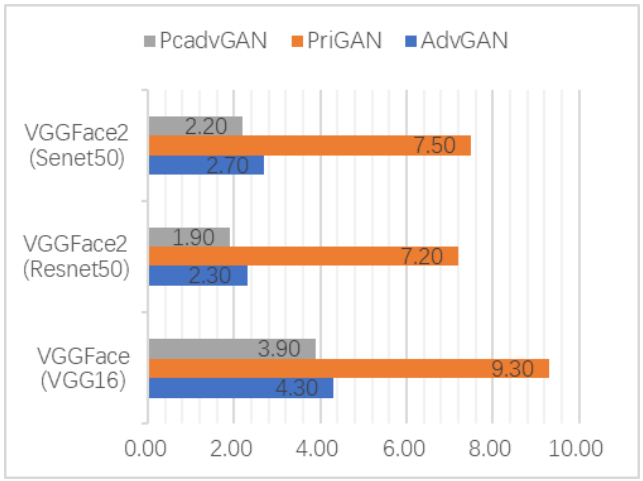

FIGURE 11. Training run times for 100 times batchsize=4, in seconds.

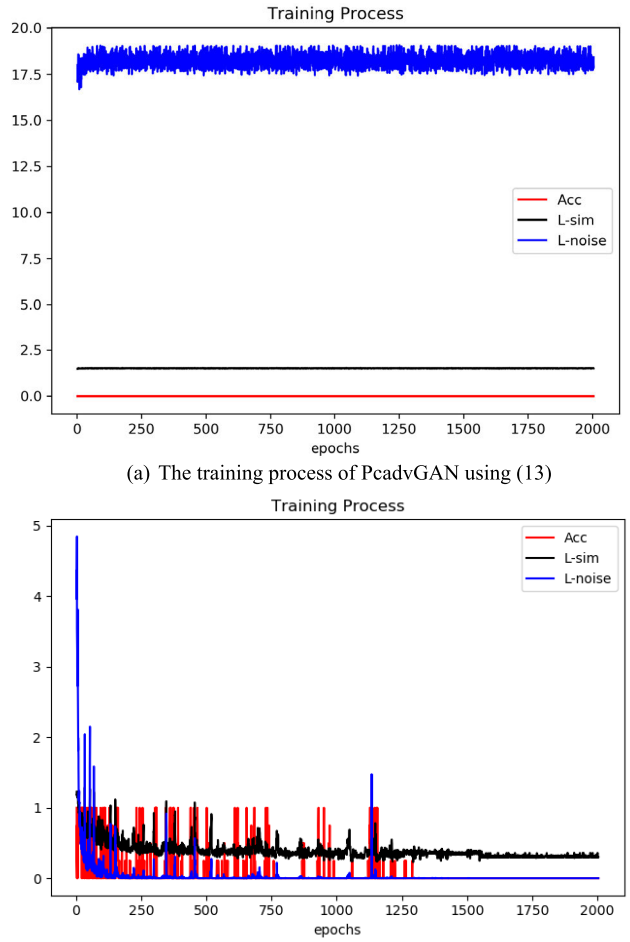

(a) The training process of PcadvGAN using (13)

(b) The training process of PcadvGAN using (14)

FIGURE 12. Training process for ablation study.

filtered by the reverse denoising algorithm, which effectively protected the privacy of the generated facial images.

The training run times of AdvGAN, PriGAN, and PcadvGAN on 100 times batchsize=4 are shown in Figure 11. As the input matrix was segmented by the proposed method and compressed twice with PCA, the input parameters were actually 0.125 times those of the original image. PcadvGAN thus runs considerably faster than AdvGAN and PriGAN. However, as image segmentation and merging operations are lengthy and additional operations (e.g., batch size and pixel comparison) are required, the actual running speed was not as high as its theoretical speed.

D. ABLATION STUDY

To confirm the contribution of the loss functions, we define two more loss functions for ablation study:

$$\mathcal{L}' = \mathcal{L}_{GAN} + \chi_1 \mathcal{L}_{adv} \tag{13}$$

$$\mathcal{L}'' = \mathcal{L}_{GAN} + \chi_1 \mathcal{L}_{adv} + \chi_2 \mathcal{L}_N \tag{14}$$

The training process of PcadvGAN using (13) and (14) iterating 2,000 epochs is shown in Figure 12. L-noise represents the size of the perturbations $\mathcal{L}_N$, and L-sim is $\mathcal{L}_{sim}$. When use loss functions (13), the values of $\mathcal{L}_N$ and $\mathcal{L}_{sim}$ stay in a high position without going down. This kind of training is totally ineffective. Due to the image proportion, the L-sim fluctuation is not obvious and actually fluctuates between 1.48 and 1.53. When use loss functions (14), $\mathcal{L}_{sim}$ reached the training bottleneck and remained stable around 0.3 in the middle and later period of training. The generated the facial privacy images can not guarantee practicability. Compared with Figure 12 and Figure 6, loss function (12) is the best way to generate the facial privacy images.

E. ROBUST

In order to test the robustness of the proposed method in this paper, PcadvGAN, AdvGAN and PriGAN are used respectively, and the target face recognition network f without defense strategy is used to generate facial privacy images, and the generated results are respectively attacked against the target face recognition network f with different defense strategies, and the results of attack success rate are shown in Table 4.

It can be seen from Table 4 that when the defense strategy of the target face recognition network adopts the median

TABLE 4. The success rate of attacking the target face recognition network *f* with defense strategy (%).

Model / Method	VGG16		Resnet50		Senet50	
	Media filter	Adv.	Media filter	Adv.	Media filter	Adv.
PcadvGan	100	22.05	100	15.62	100	6.98
AdvGan	71.16	18.75	73.34	12.50	81.66	7.22
PriGAN	68.34	6.94	73.62	2.73	77.78	3.94

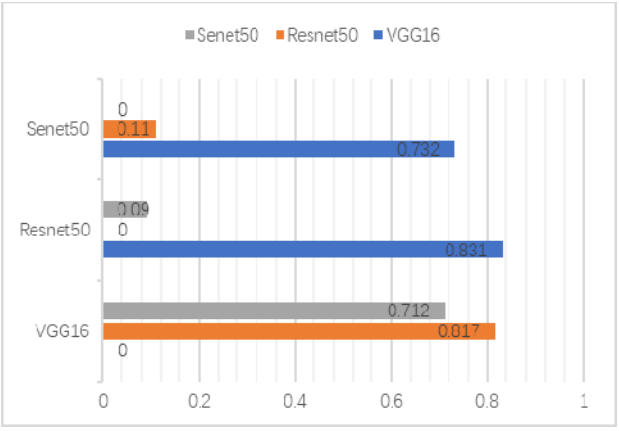

FIGURE 13. Transfer rate of adversarial samples.

filtering method, although it has a high impact on AdvGAN and PriGAN, it does not affect PcadvGAN proposed in this paper. When the defense strategy of the target face recognition network adopts the Adv. Method [37], PcadvGAN proposed in this paper is superior to the other two methods when it is VGG16 and Resnet50 network, slightly inferior to AdvGAN and superior to PriGAN when it is Senet50. It can be concluded that the PcadvGAN proposed in this paper has strong robustness than other methods.

F. EXPERIMENT AND ANALYSIS OF FACIAL IMAGES ADVERSARIAL TRANSFER EXPERIMENTS ON FACIAL PRIVACY IMAGES

Next, we used facial privacy images generated by adversarial models of VGG16, Resnet50, and Senet50 to attack the remaining two models to test for adversarial transferability in the black-box environment.

As shown in Figure 13, the SE module in Senet50 was embedded into the branch of the residual structure (which is very similar to the Resnet50 structure). The privacy of facial images trained in Resnet50 had a lower accuracy rate for recognition in Senet50 and vice versa. VGG16 differs greatly from the network structures of Resnet50 and Senet50. Hence, the transfer rate of facial privacy images trained among the three sets was low. However, as the similarity threshold of most face recognition systems is above 90%, the facial privacy images trained by PcadvGAN still have practical value.

VI. CONCLUSIONS

The paper proposes a method for protecting facial image privacy based on the principal components of the adversarial segmented image blocks. The proposed method was designed to safeguard users' privacy while ensuring the availability of their facial images. The method is superior to other similar methods in terms of image quality, running speed, and target recognition network accuracy.

ACKNOWLEDGMENT

The authors Jingjing Yang and Jiaxing Liu thank great help and encouragement from all members of the C508 Research Room, Hebei North University.

REFERENCES

[1] K. Guo, S. Wu, and Y. Xu, "Face recognition using both visible light image and near-infrared image and a deep network," *CAAI Trans. Intell. Technol.*, vol. 2, no. 1, pp. 39–47, Mar. 2017.

[2] A. Sepas-Moghaddam, P. L. Correia, and F. Pereira, "Light field local binary patterns description for face recognition," in *Proc. IEEE Int. Conf. Image Process. (ICIP)*, Beijing, China, Sep. 2017, pp. 3815–3819.

[3] J. Yang, L. Luo, J. Qian, Y. Tai, F. Zhang, and Y. Xu, "Nuclear norm based matrix regression with applications to face recognition with occlusion and illumination changes," *IEEE Trans. Pattern Anal. Mach. Intell.*, vol. 39, no. 1, pp. 156–171, Jan. 2017.

[4] G. Gao, J. Yang, X.-Y. Jing, F. Shen, W. Yang, and D. Yue, "Learning robust and discriminative low-rank representations for face recognition with occlusion," *Pattern Recognit.*, vol. 66, pp. 129–143, Jun. 2017.

[5] X. Fu, J. Lu, X. Zhang, X. Yang, and I. Unwala, "Intelligent in-vehicle safety and security monitoring system with face recognition," in *Proc. IEEE Int. Conf. Comput. Sci. Eng. (CSE), IEEE Int. Conf. Embedded Ubiquitous Comput. (EUC)*, New York, NY, USA, Aug. 2019, pp. 225–229.

[6] R. Patil, S. Patil, S. Sagar, S. Sancheti, and S. More, "Secure online payment with facial recognition using CNN," *Int. Res. J. Eng. Technol.*, vol. 6, no. 4, pp. 604–607, 2019.

[7] S. Chen, S. Ding, H. Fu, Y. Xian, X. Liu, and C. Zhang, "Deep learning applied to smart home face recognition access control system," in *Proc. 2nd Int. Conf. Artif. Intell., Technol. Appl. (ICAITA)*, Chengdu, China, 2018, pp. 13–15.

[8] W. Shen, Z. Wu, and J. Zhang, "A face privacy protection algorithm based on block scrambling and deep learning," in *Proc. Int. Conf. Cloud Comput. Secur.* Haikou, China: Springer, 2018, pp. 359–369.

[9] T. J. Schulz, "Schrems v. Data protection commissioner (CJEU)," *Int. Legal Mater.*, vol. 56, no. 2, pp. 245–272, 2017.

[10] B. Henne and M. Smith, "Awareness about photos on the Web and how privacy-privacy-tradeoffs could help," in *Proc. Int. Conf. Financial Cryptogr. Data Secur.* Okinawa, Japan: Springer, 2013, pp. 131–148.

[11] Z. Ma, Y. Liu, X. Liu, J. Ma, and K. Ren, "Lightweight privacy-preserving ensemble classification for face recognition," *IEEE Internet Things J.*, vol. 6, no. 3, pp. 5778–5790, Jun. 2019.

[12] Y. Wang and M. Kosinski, "Deep neural networks are more accurate than humans at detecting sexual orientation from facial images," *J. Personality Social Psychol.*, vol. 114, no. 2, p. 246, 2018.

[13] X. Wu and X. Zhang, "Responses to critiques on machine learning of criminality perceptions," Nov. 2016, *arXiv:1611.04135*. [Online]. Available: http://arxiv.org/abs/1611.04135

[14] W. Zeng and S. Lei, "Efficient frequency domain selective scrambling of digital video," *IEEE Trans. Multimedia*, vol. 5, no. 1, pp. 118–129, Mar. 2003.

[15] J. S. Seo, S. O. Hwang, and Y.-H. Suh, "A reversible face de-identification method based on robust hashing," in *Int. Conf. Consum. Electron. Dig. Tech. Papers*, Las Vegas, NV, USA, Jan. 2008, pp. 1–2.

[16] A. Frome, G. Cheung, A. Abdulkader, M. Zennaro, B. Wu, A. Bissacco, H. Adam, H. Neven, and L. Vincent, "Large-scale privacy protection in Google street view," in *Proc. IEEE 12th Int. Conf. Comput. Vis.*, Kyoto, Japan, Sep. 2009, pp. 2–2373.

[17] L. Meng, Z. Sun, A. Ariyaeeinia, and K. L. Bennett, "Retaining expressions on de-identified faces," in *Proc. 37th Int. Conv. Inf. Commun. Technol., Electron. Microelectron. (MIPRO)*, Opatija, Croatia, May 2014, pp. 1252–1257.

[18] L. Meng and Z. Sun, "Face de-identification with perfect privacy protection," in *Proc. 37th Int. Conv. Inf. Commun. Technol., Electron. Microelectron. (MIPRO)*, Opatija, Croatia, May 2014, pp. 1234–1239.

[19] C. Szegedy, W. Zaremba, I. Sutskever, J. Bruna, D. Erhan, I. Goodfellow, and R. Fergus, "Intriguing properties of neural networks," Dec. 2013, *arXiv:1312.6199*. [Online]. Available: http://arxiv.org/abs/1312.6199
[20] I. J. Goodfellow, J. Shlens, and C. Szegedy, "Explaining and harnessing adversarial examples," Dec. 2014, *arXiv:1412.6572*. [Online]. Available: http://arxiv.org/abs/1412.6572
[21] X. Liu, H. Yang, Z. Liu, L. Song, H. Li, and Y. Chen, "DPatch: An adversarial patch attack on object detectors," Jun. 2018, *arXiv:1806.02299*. [Online]. Available: http://arxiv.org/abs/1806.02299
[22] J. Su, D. V. Vargas, and K. Sakurai, "One pixel attack for fooling deep neural networks," *IEEE Trans. Evol. Comput.*, vol. 23, no. 5, pp. 828–841, Oct. 2019.
[23] C. Xiao, B. Li, J.-Y. Zhu, W. He, M. Liu, and D. Song, "Generating adversarial examples with adversarial networks," 2018, *arXiv:1801.02610*. [Online]. Available: http://arxiv.org/abs/1801.02610
[24] Y. He, C. Zhang, X. Zhu, and Y. Ji, "Generative adversarial network based image privacy protection algorithm," in *Proc. 10th Int. Conf. Graph. Image Process. (ICGIP)*, vol. 11069. Chengdu, China: SPIE, May 2019, Art. no. 1106927.
[25] Y. Wu, F. Yang, Y. Xu, and H. Ling, "Privacy-protective-GAN for privacy preserving face de-identification," *J. Comput. Sci. Technol.*, vol. 34, no. 1, pp. 47–60, Jan. 2019.
[26] I. T. Jolliffe and J. Cadima, "Principal component analysis: A review and recent developments," *Phil. Trans. Roy. Soc. A, Math., Phys. Eng. Sci.*, vol. 374, no. 2065, Apr. 2016, Art. no. 20150202.
[27] I. Goodfellow, J. Pouget-Abadie, M. Mirza, B. Xu, D. Warde-Farley, S. Ozair, A. Courville, and Y. Bengio, "Generative adversarial nets," in *Proc. Adv. Neural Inf. Process. Syst.*, Montreal, QC, Canada, 2014, pp. 2672–2680.
[28] M. Mirza and S. Osindero, "Conditional generative adversarial nets," Nov. 2014, *arXiv:1411.1784*. [Online]. Available: http://arxiv.org/abs/1411.1784
[29] J. Wang, X. Li, and J. Yang, "Stacked conditional generative adversarial networks for jointly learning shadow detection and shadow removal," in *Proc. IEEE/CVF Conf. Comput. Vis. Pattern Recognit.*, Salt Lake City, UT, USA, Jun. 2018, pp. 1788–1797.
[30] Y. Liu, X. Chen, C. Liu, and D. Song, "Delving into transferable adversarial examples and black-box attacks," Nov. 2016, *arXiv:1611.02770*. [Online]. Available: http://arxiv.org/abs/1611.02770
[31] O. M. Parkhi, A. Vedaldi, and A. Zisserman. (2015). *Deep Face Recognition*. [Online]. Available: https://ora.ox.ac.uk/objects/uuid:a5f2e93f-2768-45bb-8508-74747f85cad1
[32] Q. Cao, L. Shen, W. Xie, O. M. Parkhi, and A. Zisserman, "VGGFace2: A dataset for recognising faces across pose and age," in *Proc. 13th IEEE Int. Conf. Automat. Face Gesture Recognit.*, Xi'an, China, 2018, pp. 67–74.
[33] O. M. Parkhi, A. Vedaldi, and A. Zisserman. *VGG Face*. Accessed: Feb. 2020. [Online]. Available: http://www.robots.ox.ac.uk/~vgg/software/vgg_face/
[34] Q. Cao, L. Shen, W. Xie, O. M. Parkhi, and A. Zisserman. *VGGFace2 Dataset for Face Recognition*. Accessed: Mar. 2020. [Online]. Available: http://www.robots.ox.ac.uk/~vgg/data/vgg_face2/
[35] B. Liu, M. Ding, T. Zhu, Y. Xiang, and W. Zhou, "Using adversarial noises to protect privacy in deep learning era," in *Proc. IEEE Global Commun. Conf.*, Abu Dhabi, UAE, Dec. 2018, pp. 1–6.
[36] P. Linardos, S. Little, and K. McGuinness, "MediaEval 2019: Concealed FGSM perturbations for privacy preservation," 2019, *arXiv:1910.11603*. [Online]. Available: http://arxiv.org/abs/1910.11603
[37] W. He, J. Wei, X. Chen, N. Carlini, and D. Song, "Adversarial example defenses: Ensembles of weak defenses are not strong," 2017, *arXiv:1706.04701*. [Online]. Available: http://arxiv.org/abs/1706.04701
[38] X. Jin and J. Kim, "Imperceptibility improvement of image watermarking using variance selection," in *Computer Applications for Web, Human Computer Interaction, Signal and Image Processing, and Pattern Recognition*. Berlin, Germany: Springer, 2012, pp. 31–38.
[39] A. Horé and D. Ziou, "Image quality metrics: PSNR vs. SSIM," in *Proc. 20th Int. Conf. Pattern Recognit. (ICPR)*, Istanbul, Turkey, 2010, pp. 2366–2369.
[40] D. Ranganadham, P. Gorpuni, and G. Panda, "A novel fast motion estimation method based on clonal particle swarm optimization," in *Proc. Int. Conf. ICMEE*, Chennai, India, 2009, pp. 65–69.

JINGJING YANG is currently pursuing the Ph.D. degree with the Chengdu Institute of Computer Applications, Chinese Academy of Sciences. He is also an Associate Professor with the School of Information Science and Engineering, Hebei North University. His research interests include machine learning and privacy protection. He applies these techniques to a wide range of real-world problems for both academic research and industrial application. E-mail: r78z@foxmail.com.

JIAXING LIU was born in Hebei, China. He is currently pursuing the B.S. degree with the School of Information Science and Engineering, Hebei North University. His research interests include machine learning and privacy algorithm. He received many awards in China's Undergraduate Computing Application Competition. E-mail: ljx0ml@163.com.

JINZHAO WU received the Ph.D. degree from the Chinese Academy of Sciences. He is currently a Professor with Guangxi University. He is also with Guangxi University for Nationalities. He has provided consulting to many major companies worldwide. He has been engaged in the research and development of efficient and highly reliable computing and reasoning theories and tools. He has published three books and more than 100 refereed articles. His research interests include symbol computing, automatic reasoning, machine learning, formal methods, and their intersection, fusion, and application.